ACS Medicinal Chemistry Letters

Letter

Synthesis and Automated Labeling of [18F]Darapladib, a Lp-PLA2 ligand, as potential PET Imaging tool of Atherosclerosis

Florian Guibbal, Vincent Meneyrol, Imade Ait-Arsa, Nicolas Diotel, Jessica Patche, Bryan Veeren, Sébastien Bénard, Fanny Gimie, Jennyfer Yong-Sang, Ilya Khantalin, Reuben Veerapen, Emmanuelle Jestin, and Olivier Meilhac

ACS Med. Chem. Lett., **Just Accepted Manuscript** • DOI: 10.1021/acsmedchemlett.8b00643 • Publication Date (Web): 04 Apr 2019

Just Accepted

ACS Publications

is published by the American Chemical Society. 1155 Sixteenth Street N.W., Washington, DC 20036

Synthesis and Automated Labeling of [^{18}F]Darapladib, a Lp-PLA$_2$ ligand, as potential PET Imaging tool of Atherosclerosis

Florian Guibbal[1], Vincent Meneyrol[2], Imade Ait-Arsa[2], Nicolas Diotel[1], Jessica Patché[1], Bryan Veeren[1], Sébastien Bénard[2], Fanny Gimié[2], Jennyfer Yong-Sang[1], Ilya Khantalin[3], Reuben Veerapen[4], Emmanuelle Jestin[1,2] and Olivier Meilhac[1,3]*

(1) Université de La Réunion, INSERM, UMR 1188 Diabète athérothrombose Thérapies Réunion Océan Indien (DéTROI), Saint-Denis de La Réunion, France

(2) CYclotron Réunion Océan Indien CYROI, 2 rue Maxime Rivière, 97490 Sainte-Clotilde

(3) CHU de La Réunion, Saint-Denis de La Réunion, France

(4) Clinique de Sainte-Clotilde, 127, Route de Bois de Nèfles, Sainte-Clotilde, Réunion, France

ABSTRACT: Atherosclerosis and its associated clinical complications are major health issues in industrialized countries. Lp-PLA$_2$ (Lipoprotein-associated phospholipase A$_2$) was demonstrated to play an important role in atherogenesis and to be a potential risk prediction factor of plaque rupture. Darapladib is one of the most potent Lp-PLA$_2$ inhibitors with an IC$_{50}$ of 0.25 nM. Using its affinity for Lp-PLA$_2$, we describe herein the total synthesis of darapladib radiolabeling precursor and the automated radiolabeling process for PET imaging *via* an arylboronate moiety. The tracer thus obtained was tested in a mouse model of atherosclerosis (ApoE KO) and compared with the widely used [^{18}F]FDG PET tracer, known to label metabolically active cells. [^{18}F]Darapladib showed a significant accumulation within mice aortic atheromatous plaques dissected out *ex vivo* compared to [^{18}F]FDG. Incubation of the radiotracer with human carotid samples showed a strong accumulation within the atherosclerotic plaques and supports its potential for use in PET imaging.

KEYWORDS : Atherosclerosis, darapladib, PET imaging, Lp-PLA$_2$, automated radiofluorination, aryl boronate

In western countries, cardiovascular diseases and in particular atherosclerotic complications are responsible for about 50% of death.[1] Atherosclerosis is characterized by an accumulation of lipids and inflammatory cells within the vascular wall of large arteries.[2] In spite of important therapeutic progresses, fatal events due to atherosclerotic diseases remain a growing public health issue. Increasing efforts are made to find new non-invasive imaging tools to assess plaque localization, composition and susceptibility to rupture.[3] Functional molecular imaging can enable early detection of disease and assessment of therapy efficacy. Positron emission tomography (PET) has become a powerful tool to diagnose disorders including cancer,[4] neurological[5] or heart diseases.[6] Fluorine-18 is the most widely used radioisotope for PET diagnosis due to its relatively short half-life ($t_{1/2}$ = 109.8 min), high spatial resolution imaging and covalent radiolabeling.[7,8] In nuclear medicine, [^{18}F]fluorodeoxyglucose or [^{18}F]FDG is the most successful radiopharmaceutical used for PET diagnosis based on the increased metabolic demand of cells, particularly in oncology. However, [^{18}F]FDG use for detection of atherosclerosis presents some limitations due to the heterogeneity of glucose consumption by vascular and inflammatory cells.[9] There is an important need for identification of vulnerable plaques, prone to rupture. In atherosclerotic plaques, lipoprotein-associated phospholipase A$_2$ (Lp-PLA$_2$) is a well-established biomarker associated with the accumulation of both low-density lipoproteins (LDL) and inflammatory cells such as macrophages.[10] The pro-inflammatory properties of this enzyme have been associated to its ability to efficiently hydrolyze oxidized phospholipids, leading to the formation of lysophosphatidylcholine and oxidized free fatty acids.[11] Lp-PLA$_2$ activity and presence could represent useful biomarkers to identify cardiovascular diseases and offer a potent therapeutic alternative to known methods through Lp-PLA$_2$ inhibition.[12] This enzyme has been targeted by pharmaceutical groups in order to develop specific inhibitors.[13,14,15,16] Darapladib was developed by GSK as the most potent Lp-PLA$_2$ inhibitor (IC$_{50}$ = 0.25 nM, using human recombinant enzyme).[17] Since critical endpoints were not met (cardiovascular death, coronary events, myocardial infarction and stroke) in both STABILITY and SOLID-TIMI 52 studies, darapladib failed to pass phase III clinical trials.[18,19,20] Taking advantage of the strong affinity of darapladib for Lp-PLA$_2$,[21,22] the demonstrated *in vivo* safety and the presence of a fluorine in its structure, we used [^{18}F]darapladib to target atherosclerotic plaques by PET imaging.

Chart 1. **Four moieties of darapladib involved in Lp-PLA$_2$ recognition. Groups 1 and 2 are mainly involved in binding to Lp-PLA$_2$ catalytic site. Red arrow: targeted site for ^{18}F-radiolabeling.**

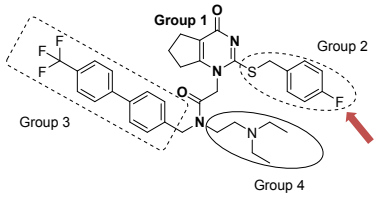

Since the original structure of darapladib (**Chart 1**) is preserved, both physico-chemical properties (solubility, polarity, etc.) and *in vivo* behavior (metabolism, catabolism,

etc.) of the radioactive molecule will be similar to the native compound. As shown in **Chart 1**, in order to ^{18}F-radiolabel darapladib on the aryl position of group 2, we chose to synthesize an aryl-boronate precursor. SNAr reactions are the most widely used methods to produce ^{18}F-labeled arenes. There are two main strategies available to perform radiofluorination of arenes, devoid of strong electron-withdrawing groups.[23] The first involves the radiofluorination of strong electrophiles such as iodonium ylides[24] or diaryliodonium salts.[25] However, with electron neutral arenes, these reactions require high temperature and offer low radiochemical yields (RCY).[24] To address these limitations, a second strategy was initiated by Scott *et al*.[26] They proposed, under mild conditions, the use of K^{18}F to obtain ^{18}F-labeled electron-rich, neutral, and deficient aryl fluorides. Shortly after, Gouverneur *et al*.[27,28] offered a new pathway that targets direct nucleophilic ^{18}F-fluorination of a wide range of arylboronate esters with K^{18}F/K$_{222}$ mediated by the commercially available copper complex [Cu(OTf)$_2$(Py)$_4$]. Scott *et al*. then proposed an alternative that directly forms, *in situ*, the copper complex.[29] This method allows more constant radiochemical yields and radiofluorination of both boronates and boronic acid derivatives. We report herein the synthesis of ^{18}F-radiolabeled darapladib via alcohol-enhanced Cu-mediated radiofluorination[30] (**Scheme 1**) in order to image atherosclerotic plaques. K$_{222}$ was excluded from our automated method since its use was demonstrated to be detrimental to reaction yields.[31] We used our previously reported darapladib synthesis method in order to produce the radiofluorination precursor. Darapladib biphenyl moiety and aliphatic chain (respectively groups 3 and 4) were obtained as previously described.[32]

Scheme 1. Copper-mediated radiofluorination of aryl boronates.

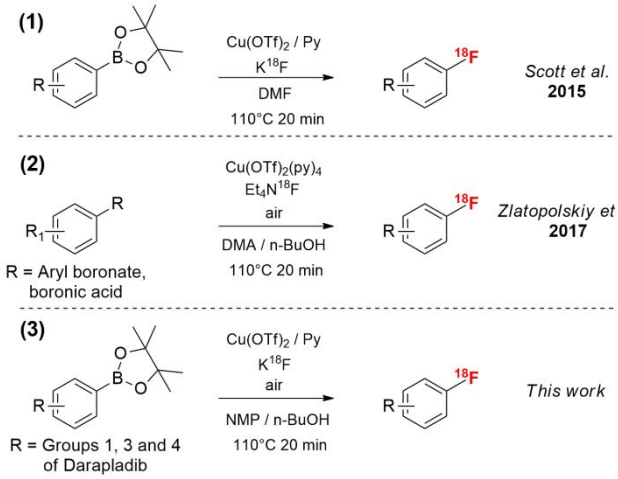

(1) Scott *et al*. pathway with formation of the copper complex in situ. (2) Zlatopolskiy *et al*. alcohol-enhanced radiofluorination with 30% alcohol charge. (3) Radiolabeling strategy for [^{18}F]darapladib consisting in both *in situ* complex formation and 30% alcohol charge.

We first synthetized the arylboronate moiety that will allow ^{18}F-labeling (**Scheme 2**). 4-bromobenzaldehyde was reduced to the corresponding alcohol **1** in 91% yield. In a palladium-catalyzed coupling, the boronate moiety was inserted in 91% followed by bromination via CBr$_4$ to obtain **3** in 94% yield. As shown in **Scheme 3**, we then synthetized the radiolabeling boronate precursor **9** of darapladib. Thiouracile **4** was synthetized as previously described[32] and engaged in a substitution with alkylating agent **3** to afford compound **5** in 98% yield.

Scheme 2. Synthesis of boronate derivative 3.

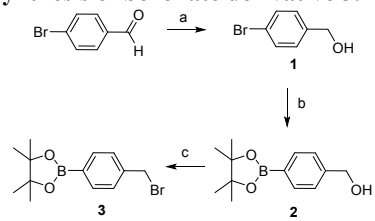

Reagents and conditions: (a) NaBH$_4$, THF/MeOH 7/3, 0°C for 30 min; (b) KOAc, bis(pinacolato)diboron, Pd(dppf)Cl$_2$, DMSO, 85°C for 18h; (c) CBr$_4$, PPh$_3$, THF, RT for 18h.

Non-selective alkylation with *tert*-butyl-bromoacetate yielded the desired *N1*-ester **6** (26%) which was then hydrolyzed with TFA using a carbocation scavenger (TIS) to afford acid **7** (64%). Peptide coupling of **8** (previously described)[32] and **7** allowed us to obtain darapladib-arylboronate radiolabeling precursor **9** in 70% yield.

Scheme 3. Synthesis of the radiolabeling precursor 9.

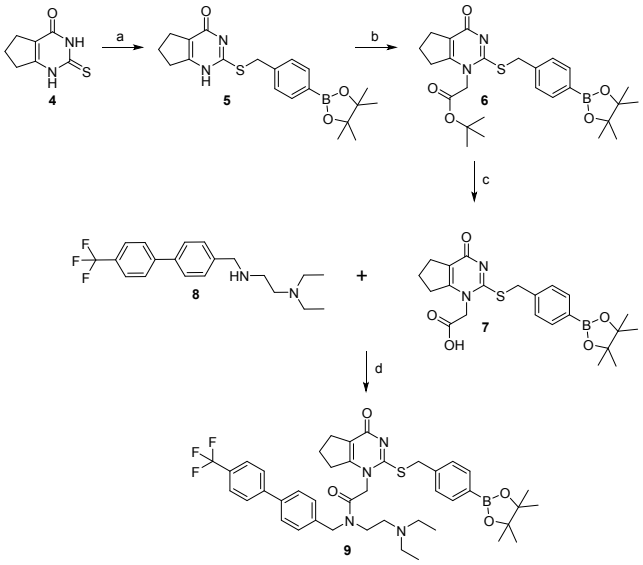

Reagents and conditions: (a) KI, K$_2$CO$_3$, **3**, acetone, 54°C for 3h; (b) *tert*-butyl-bromoacetate, DIPEA, DCM, 40°C for 20h; (c) TFA, TIS, DCM, RT for 20h; (d) COMU, DIPEA, DMF, 0°C for 1h then RT for 12h.

The precursor **9** was then engaged in a copper-mediated aryl-radiofluorination using a GE Healthcare TRACERlab FX FN module (**Scheme 4**). Initially, we worked under Scott *et al*. conditions in order to produce radiolabeled darapladib. Elution of ^{18}F- from anion exchanger QMA cartridge was performed using a KOTf/K$_2$CO$_3$ aqueous solution (5 mg/50 µg in 550 µL). The eluted fluorine was azeotropically dried with acetonitrile (60°C then 120°C) since copper-mediated labeling showed water sensitivity.[29] Reactions were carried out at 110°C under vacuum for 20 min. Gouverneur *et al*. explain that the copper complex might need to be re-oxidized since highly reactive copper(III) species may be responsible for the SNAr reaction. Thus, air was injected 4 times during the reaction course since very low yields (<1%) were obtained without air addition. The reaction mixture was then loaded on preparative HPLC for purification after passing through a Sep-Pak Alumina N cartridge and then formulated in a 5% EtOH saline solution. As presented in **Table 1**, radiofluorination in DMF produced the desired radiotracer in a very low yield (**entry 1**) and NMP did not provide any significant improvement (**entry 2**), both methods leading to a maximum of 1% recovery.

Scheme 4. Radiosynthesis of [^{18}F]darapladib from 9.

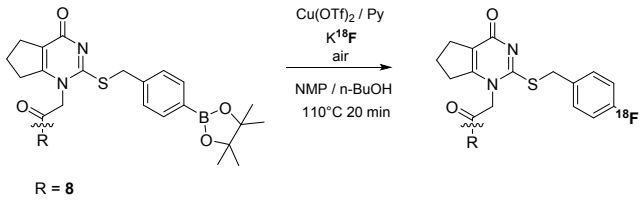

In 2017, Zlatopolskiy *et al*. proposed an alcohol-enhanced copper-mediated radiofluorination that replaced water azeotropic removal by eluting Et_4NHCO_3 in n-BuOH of QMA-trapped $^{18}F^-$. They also showed that the use of NMP offered a better yield than DMF with 30% alcohol charge. In our hands, $^{18}F^-$ elution using n-BuOH did not offer sufficient yields (less than 20% of the starting activity). We thus kept our eluting conditions, which offered a better $^{18}F^-$ yield (up to 95%). Compound **9** was dissolved in a 990 µL mixture of NMP/n-BuOH (0.6/0.3; v/v) and was added to the reactor containing previously dried $^{18}F^-$. This protocol allowed us to increase [^{18}F]darapladib radiofluorination up to 6% (**entries 3** and **4**). Automated radiofluorination RCY obtained were similar or even better than those reported in the literature for automated copper-mediated ^{18}F-radiofluorination. The final solutions concentrations were around 200 ± 50 MBq/mL that are suitable for preclinical studies requirements.[33]

Table 1. Copper-mediated radiofluorination of 9.

Entry	Solvents	Activity (MBq)[a]	RCY[b]
1	DMF	257	<1%
2	NMP	379	1%
3	NMP / n-BuOH[c]	2310	6%
4	NMP / n-BuOH[c]	1979	5%

[a] Before formulation process; [b] Decay corrected; [c] Starting activity: 58 000 MBq (**entry 3**), 52 000 MBq (**entry 4**).

[^{18}F]Darapladib purity (>99%) and specific activity (40-60 GBq/µmol) were assessed by radio-HPLC (see supporting information). Radiolabeled darapladib retention time was similar to the cold reference [^{19}F]darapladib and no radioactive contaminants were detected. [^{18}F]Darapladib stability (see supporting information) was confirmed in saline buffer at 0, 30 and 90 min with no degradation observed. In order to evaluate the ability of [^{18}F]darapladib to target atherosclerotic plaques, the radiotracer was injected in a mouse model known to develop aortic atheroma plaques (Apolipoprotein E- deficient or ApoE KO mice) and compared to wild type C57BL/6 mice. [^{18}F]Darapladib was compared to [^{18}F]FDG, which was suggested to label inflammation associated with atherosclerotic plaques.[34] 15 ± 5 MBq syringes of [^{18}F]darapladib or [^{18}F]FDG were injected via the caudal vein in 10 month-old ApoE KO and C57BL/6 mice. Since no differences were observed between 15 and 45 min acquisitions, the optimal imaging time was set at 15 min for subsequent experiments. Whole body imaging did not allow us to localize [^{18}F]darapladib in the aorta, due to the high uptake by other organs such as liver (19 ± 2 %ID/g), intestines (32 ± 1 %ID/g) and kidneys (21 ± 1 %ID/g) (see supporting information). Injection in C57BL/6 wild type mice led to a similar uptake in these major organs liver (23 ± 3 %ID/g), intestines (26 ± 5 %ID/g) and kidneys (11 ± 4 %ID/g) but nothing was observable in the aorta. [^{18}F]Darapladib accumulated mainly in the liver, kidneys and intestines, suggesting a binding to LDL/HDL-associated Lp-PLA_2, since these organs are involved in lipoprotein metabolism.[33] These results were supported by immunohistochemistry staining with anti-Lp-PLA2 antibody (see supporting information) showing the presence of our target in livers. Accumulation within kidneys and intestines were already explained by Dave and co-workers.[35]

Figure 1. ***Ex vivo*** **aorta and heart PET imaging of [^{18}F]darapladib and [^{18}F]FDG in ApoE KO and C57BL/6 mice.**

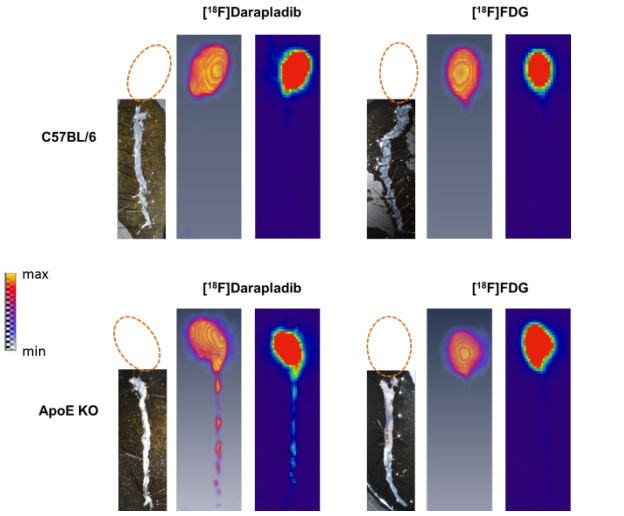

The heart was removed for dissection of the aorta; its position is indicated with an orange dashed circle. From left to right: macroscopic picture, 3D view, 2D slice.

In comparison, [^{18}F]FDG accumulated in high-glucose consuming organs (brain/heart) and in kidneys and bladder, as they are involved in glucose catabolism. To evaluate [^{18}F]darapladib accumulation within atheromatous vessels, the heart and aorta were dissected out 15 min post-injection, flushed with saline and imaged *ex vivo* (15 min PET acquisition) (**Figure 1**). The aortas were then opened longitudinally, split and pined onto a black wax surface, in order to expose the atheromatous plaques. *Ex vivo* PET images were compared to macroscopic captures of atheromatous plaques. No accumulation was observed in the aorta for either [^{18}F]darapladib or [^{18}F]FDG in C57BL/6 mice (below detection threshold), devoid of plaques (**Figure 1**). In contrast, a strong labeling of the aorta was observed in ApoE KO mice with [^{18}F]darapladib (4.6 ± 0.8 %ID/g) but not with [^{18}F]FDG (below detection threshold). This suggests that darapladib may represent a good radiotracer for detection of atheromatous plaques. These results were comforted by immunohistochemistry staining showing the high presence of Lp-PLA_2 within mice aortas and aortic sinuses (see supporting information). In order to consolidate these results, we tested the ability of [^{18}F]darapladib to label human carotid atherosclerotic samples known to exhibit high level of Lp-PLA_2. Both [^{18}F]darapladib and [^{18}F]FDG were tested *ex vivo* in freshly obtained carotid endarterectomy samples (**Figure 2**). Our previously reported study showed that excised tissue is still alive and metabolically active.[36] As depicted in **Figure 2**, [^{18}F]FDG-incubated carotid samples displayed a weak signal only in the stenosed complicated plaque sample (0.02 %ID/g for culprit and 0.01 %ID/g for non-complicated plaques). More

interestingly, [^{18}F]darapladib was able to significantly accumulate in both complicated and non-complicated parts of atherosclerotic carotid samples ten times higher than [^{18}F]FDG (0.1 %ID/g for both culprit and non-complicated plaques). This highlights that, using our ^{18}F-labeled ligand, accumulation of Lp-PLA$_2$ associated with lipoproteins and monocytes/macrophages may represent an interesting target for imaging sub-clinical atherosclerosis. Immunohistochemistry for detection of Lp-PLA$_2$ was performed on the same samples (see supporting information) and a strong staining was observed on both complicated and non-complicated parts, supporting the hypothesis that [^{18}F]darapladib binds Lp-PLA$_2$ in human endarterectomy samples. These results were supported by DESI-IMS studies that show association between the presence of [^{19}F]darapladib and Lp-PLA$_2$ after incubation of carotid samples with the cold compound (see supporting information). Since [^{18}F]darapladib seems to be more effective than [^{18}F]FDG for imaging inflammatory cells in atherosclerosis, we tested its ability to accumulate in tumors, also known to contain monocytes/macrophages.

Figure 2. ***Ex vivo*** **accumulation of [^{18}F]darapladib compared to [^{18}F]FDG in human carotid samples.**

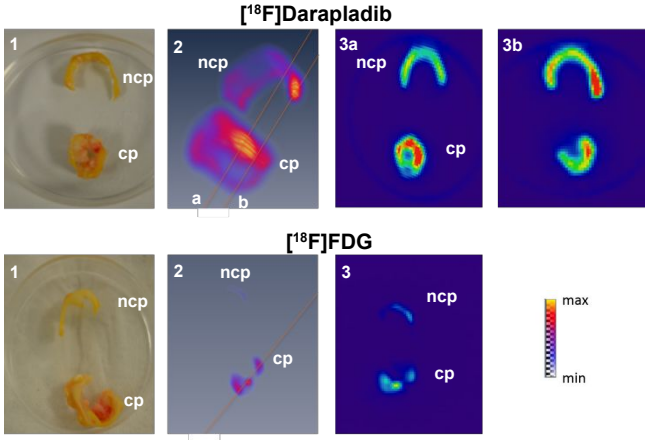

1) Macroscopic view (ncp: non-complicated plaque, cp: culprit plaque corresponding to the stenosed part of the same carotid sample; 2) 3D PET imaging view showing slice planes a and b in orange; 3) corresponding orthoslice of plans a and b.

Radiolabeled darapladib or [^{18}F]FDG (15 ± 5 MBq) were injected via the caudal vein in melanoma B16-injected mice that develop tumors (see supporting information).[34] As expected, [^{18}F]FDG provided an intense radiolabeling of tumors whereas [^{18}F]darapladib imaging was surprisingly negative in this model (its accumulation was observed only in the liver, kidney and intestines). These results suggest a better specificity of [^{18}F]darapladib than [^{18}F]FDG for detection of atheromatous plaques. The cells composing the plaque may have a lower glucose uptake than cancer cells. In contrast, the presence of Lp-PLA$_2$-expressing cells such as macrophages and lipoproteins provide good targets for [^{18}F]darapladib.

We have described the synthesis of the radiolabeling precursor of darapladib. Through aryl-boronate pathway, we were able to perform copper-mediated ^{18}F-labeling of darapladib on an automated module (n = 10) with good radiochemical purity assessed by radio-HPLC (>99%) and specific activity (40-60 GBq/µmol). Although the sensitivity of micro-PET did not allow us to detect small atheromatous plaques *in vivo*, PET studies performed with [^{18}F]FDG and [^{18}F]Darapladib showed a good affinity of our labeled Lp-PLA$_2$ ligand for atheromatous plaques relative to [^{18}F]FDG that was more specific for tumor detection. The suitability of [^{18}F]darapladib for detection of Lp-PLA$_2$ within atherosclerotic plaques was confirmed in human samples. Although RCY and specific activities may be improved, the use of [^{18}F]darapladib for imaging in clinical settings could be of interest, in particular since phase I and II clinical trials reported darapladib use in Humans.[37] Further investigations would be needed to assess the specificity of [^{18}F]Darapladib in other preclinical models using bigger animals (i.e rabbits or pigs) and to confirm its safety for imaging trials.

AUTHOR INFORMATIONS

Corresponding Author

Phone: +(262) 262 938 811. E-mail: olivier.meilhac@inserm.fr

Author Contributions

The manuscript was written through contributions of all authors. All authors have given approval to the final version of the manuscript.

Funding Sources

This work was supported by the ERDF (European Regional Development Fund) 33054 and RE0001897 (EU- Région Réunion -French State national counterpart) as well as a Philancia fund. Florian Guibbal was supported by a CIFRE doctoral grant n°2013/1522.

Acknowledgments

This work has benefited from the facilities and expertise of the Small Molecule Mass Spectrometry platform of ICSN and NMR service (Centre de Recherche de Gif-www.icsn.cnrs-gif.fr).

Abbreviations

COMU ((1-Cyano-2-ethoxy-2-oxoethylidenaminooxy) dimethyl aminomorpholino-carbenium hexafluorophosphate), DCM (dichloromethane), DESI-IMS (desorption electrospray ionization - ion mobility spectrometry), DIPEA (N,N-Diisopropylethylamine), DMA (dimethylacetamide), DMF (N,N-dimethylformamide), DMSO (dimethyl sulfoxide), FDG (Fluorodeoxyglucose), GSK (Glaxo Smith Kline), HDL (high density lipoprotein), LDL (low density lipoprotein), NMP (N-methyl-2-pyrrolidone), Py (pyridine), QMA (quaternary methyl ammonium), Tf (triflate), TFA (trifluoro acetic acid), THF (tetrahydrofuran), TIS (triisopropyl silane), PET (positron emission tomography), RCY (radiochemical yield).

Supporting information

Chemistry, radiochemistry and imaging experimental procedures, NMR spectra. FX-FN module, stabilities and biodistribution studies. DESI-MS and IHC studies.

References

1. WHO Cardiovascular diseases (CVDs). http://www.who.int/mediacentre/factsheets/fs317/en/ (09/05).
2. Ross, R. Atherosclerosis--an inflammatory disease, *N. Engl. J. Med.* **1999**, *340* (2), 115-126.
3. Zoghbi, W. A. Cardiovascular Imaging: A Glimpse Into The Future, *Methodist DeBakey Cardiovasc. J.* **2014**, *10* (3), 139-145.
4. Saif, M. W.; Tzannou, I.; Makrilia, N.; Syrigos, K. Role and cost effectiveness of PET/CT in management of patients with cancer, *Yale J. Biol. Med.* **2010**, *83* (2), 53-65.
5. Maher-Edwards, G.; De'Ath, J.; Barnett, C.; Lavrov, A.; Lockhart, A. A 24-week study to evaluate the effect of rilapladib on cognition and

cerebrospinal fluid biomarkers of Alzheimer's disease, *Alzheimer's Dementia: Transl. Res. Clin. Interventions.* **2015**, *1* (2), 131-140.
6. Kajander, S.; Joutsiniemi, E.; Saraste, M.; Pietilä, M.; Ukkonen, H.; Saraste, A.; Sipilä, H. T.; Teräs, M.; Mäki, M.; Airaksinen, J.; Hartiala, J.; Knuuti, J. Cardiac positron emission tomography/computed tomography imaging accurately detects anatomically and functionally significant coronary artery disease, *Circulation* **2010**, *122* (6), 603-613.
7. Le Bars, D. Fluorine-18 and medical imaging: Radiopharmaceuticals for positron emission tomography, *J. Fluorine Chem.* **2006**, *127* (11), 1488-1493.
8. Wenzel, B.; Mollitor, J.; Deuther-Conrad, W.; Dukic-Stefanovic, S.; Kranz, M.; Vraka, C.; Teodoro, R.; Günther, R.; Donat, C. K.; Ludwig, F.-A.; Fischer, S.; Smits, R.; Wadsak, W.; Mitterhauser, M.; Steinbach, J.; Hoepping, A.; Brust, P. Development of a Novel Nonpeptidic (18)F-Labeled Radiotracer for in Vivo Imaging of Oxytocin Receptors with Positron Emission Tomography, *J. Med. Chem.* **2016**, *59* (5), 1800-1817.
9. Almuhaideb, A.; Papathanasiou, N.; Bomanji, J. 18F-FDG PET/CT imaging in oncology, *Ann. Saudi Med.* **2011**, *31* (1), 3-13.
10. Cai, A.; Zheng, D.; Qiu, R.; Mai, W.; Zhou, Y. Lipoprotein-associated phospholipase A2 (Lp-PLA(2)): a novel and promising biomarker for cardiovascular risks assessment, *Dis. Markers* **2013**, *34* (5), 323-331.
11. Zalewski, A.; Macphee, C. Role of lipoprotein-associated phospholipase A2 in atherosclerosis: biology, epidemiology, and possible therapeutic target, *Arterioscler. Thromb. Vasc. Biol.* **2005**, *25* (5), 923-931.
12. Karakas, M.; Koenig, W. Lp-PLA2 Inhibition—The Atherosclerosis Panacea, *Pharmaceuticals* **2010**, *3* (5), 1360-1373.
13. Wang, K.; Xu, W.; Zhang, W.; Mo, M.; Wang, Y.; Shen, J. Triazole derivatives: a series of Darapladib analogues as orally active Lp-PLA2 inhibitors, *Bioorg. Med. Chem. Lett.* **2013**, *23* (10), 2897-2901.
14. Nagano, J. M.; Hsu, K. L.; Whitby, L. R.; Niphakis, M. J.; Speers, A. E.; Brown, S. J.; Spicer, T.; Fernandez-Vega, V.; Ferguson, J.; Hodder, P.; Srinivasan, P.; Gonzalez, T. D.; Rosen, H.; Bahnson, B. J.; Cravatt, B. F. Selective inhibitors and tailored activity probes for lipoprotein-associated phospholipase A(2), *Bioorg. Med. Chem. Lett.* **2013**, *23* (3), 839-843.
15. Wang, Y.; Xu, W.; Shao, H.; Xie, Y.; Wang, J. Design and Synthesis of Novel Pyrazole-based Lp-PLA2 Inhibitors, *Chin. J. Chem.* **2011**, *29* (10), 2039-2048.
16. Wang, K.; Xu, W.; Liu, Y.; Zhang, W.; Wang, W.; Shen, J.; Wang, Y. Design and synthesis of imidazole and triazole derivatives as Lp-PLA_2 inhibitors and the unexpected discovery of highly potent quaternary ammonium salts, *Bioorg. Med. Chem. Lett.* **2013**, *23* (5), 1187-1192.
17. Blackie, J. A.; Bloomer, J. C.; Brown, M. J. B.; Cheng, H.-Y.; Hammond, B.; Hickey, D. M. B.; Ife, R. J.; Leach, C. A.; Lewis, V. A.; Macphee, C. H.; Milliner, K. J.; Moores, K. E.; Pinto, I. L.; Smith, S. A.; Stansfield, I. G.; Stanway, S. J.; Taylor, M. A.; Theobald, C. J. The identification of clinical candidate SB-480848: a potent inhibitor of lipoprotein-associated phospholipase A2, *Bioorg. Med. Chem. Lett.* **2003**, *13* (6), 1067-1070.
18. White, H.; Held, C.; Stewart, R.; Watson, D.; Harrington, R.; Budaj, A.; Steg, P. G.; Cannon, C. P.; Krug-Gourley, S.; Wittes, J.; Trivedi, T.; Tarka, E.; Wallentin, L. Study design and rationale for the clinical outcomes of the STABILITY Trial (STabilization of Atherosclerotic plaque By Initiation of darapLadIb TherapY) comparing darapladib versus placebo in patients with coronary heart disease, *Am. Heart J.* **2010**, *160* (4), 655-661.
19. O'Donoghue, M. L.; Braunwald, E.; White, H. D.; Lukas, M. A.; Tarka, E.; Steg, P. G.; Hochman, J. S.; Bode, C.; Maggioni, A. P.; Im, K.; Shannon, J. B.; Davies, R. Y.; Murphy, S. A.; Crugnale, S. E.; Wiviott, S. D.; Bonaca, M. P.; Watson, D. F.; Weaver, W. D.; Serruys, P. W.; Cannon, C. P.; Investigators, S.-T.; Steen, D. L. Effect of darapladib on major coronary events after an acute coronary syndrome: the SOLID-TIMI 52 randomized clinical trial, *JAMA* **2014**, *312* (10), 1006-1015.
20. Investigators, S.; White, H. D.; Held, C.; Stewart, R.; Tarka, E.; Brown, R.; Davies, R. Y.; Budaj, A.; Harrington, R. A.; Steg, P. G.; Ardissino, D.; Armstrong, P. W.; Avezum, A.; Aylward, P. E.; Bryce, A.; Chen, H.; Chen, M. F.; Corbalan, R.; Dalby, A. J.; Danchin, N.; De Winter, R. J.; Denchev, S.; Diaz, R.; Elisaf, M.; Flather, M. D.; Goudev, A. R.; Granger, C. B.; Grinfeld, L.; Hochman, J. S.; Husted, S.; Kim, H. S.; Koenig, W.; Linhart, A.; Lonn, E.; Lopez-Sendon, J.; Manolis, A. J.; Mohler, E. R., 3rd; Nicolau, J. C.; Pais, P.; Parkhomenko, A.; Pedersen, T. R.; Pella, D.; Ramos-Corrales, M. A.; Ruda, M.; Sereg, M.; Siddique, S.; Sinnaeve, P.; Smith, P.; Sritara, P.; Swart, H. P.; Sy, R. G.; Teramoto, T.; Tse, H. F.; Watson, D.; Weaver, W. D.; Weiss, R.; Viigimaa, M.; Vinereanu, D.; Zhu, J.; Cannon, C. P.; Wallentin, L. Darapladib for Preventing Ischemic Events in Stable Coronary Heart Disease, *N. Engl. J. Med.* **2014**, *370* (18), 1702-1711.
21. Woolford, A. J. A.; Pero, J. E.; Aravapalli, S.; Berdini, V.; Coyle, J. E.; Day, P. J.; Dodson, A. M.; Grondin, P.; Holding, F. P.; Lee, L. Y. W.; Li, P.; Manas, E. S.; Marino, J.; Martin, A. C. L.; McCleland, B. W.; McMenamin, R. L.; Murray, C. W.; Neipp, C. E.; Page, L. W.; Patel, V. K.; Potvain, F.; Rich, S.; Rivero, R. A.; Smith, K.; Somers, D. O.; Trottet, L.; Velagaleti, R.; Williams, G.; Xie, R. Exploitation of a Novel Binding Pocket in Human Lipoprotein-Associated Phospholipase A2 (Lp-PLA2) Discovered through X-ray Fragment Screening, *J. Med. Chem.* **2016**, *59* (11), 5356-5367.
22. Liu, Q.; Chen, X.; Chen, W.; Yuan, X.; Su, H.; Shen, J.; Xu, Y. Structural and Thermodynamic Characterization of Protein–Ligand Interactions Formed between Lipoprotein-Associated Phospholipase A2 and Inhibitors, *J. Med. Chem.* **2016**, *59* (10), 5115-5120.
23. Merritt, E. A.; Olofsson, B. Diaryliodonium salts: a journey from obscurity to fame, *Angew. Chem. Int. Ed.* **2009**, *48* (48), 9052-9070.
24. Rotstein, B. H.; Stephenson, N. A.; Vasdev, N.; Liang, S. H. Spirocyclic hypervalent iodine(III)-mediated radiofluorination of non-activated and hindered aromatics, *Nat. Commun.* **2014**, *5*, 4365.
25. Pike, V. W.; Aigbirhio, F. I. Reactions of cyclotron-produced [18F]fluoride with diaryliodonium salts—a novel single-step route to no-carrier-added [18]fluoroarenes, *J. Chem. Soc., Chem. Commun.* **1995**, *21*, 2215-2216.
26. Ichiishi, N.; Brooks, A. F.; Topczewski, J. J.; Rodnick, M. E.; Sanford, M. S.; Scott, P. J. H. Copper-Catalyzed [18F]Fluorination of (Mesityl)(aryl)iodonium Salts, *Org. Lett.* **2014**, *16* (12), 3224-3227.
27. Tredwell, M.; Preshlock, S. M.; Taylor, N. J.; Gruber, S.; Huiban, M.; Passchier, J.; Mercier, J.; Genicot, C.; Gouverneur, V. A general copper-mediated nucleophilic 18F fluorination of arenes, *Angew. Chem. Int. Ed.* **2014**, *53* (30), 7751-7755.
28. Taylor, N. J.; Emer, E.; Preshlock, S.; Schedler, M.; Tredwell, M.; Verhoog, S.; Mercier, J.; Genicot, C.; Gouverneur, V. Derisking the Cu-Mediated 18F-Fluorination of Heterocyclic Positron Emission Tomography Radioligands, *J. Am. Chem. Soc.* **2017**, *139* (24), 8267-8276.
29. Mossine, A. V.; Brooks, A. F.; Makaravage, K. J.; Miller, J. M.; Ichiishi, N.; Sanford, M. S.; Scott, P. J. H. Synthesis of [^{18}F]Arenes via the Copper-Mediated [^{18}F]Fluorination of Boronic Acids, *Org. Lett.* **2015**, *17* (23), 5780-5783.
30. Zischler, J.; Kolks, N.; Modemann, D.; Neumaier, B.; Zlatopolskiy, B. D. Alcohol-Enhanced Cu-Mediated Radiofluorination, *Chemistry* **2017**, *23* (14), 3251-3256.
31. Mossine, A. V.; Brooks, A. F.; Ichiishi, N.; Makaravage, K. J.; Sanford, M. S.; Scott, P. J. H. Development of Customized [18F]Fluoride Elution Techniques for the Enhancement of Copper-Mediated Late-Stage Radiofluorination, *Sci. Rep.* **2017**, *7*.
32. Guibbal, F.; Bénard, S.; Patché, J.; Meneyrol, V.; Couprie, J.; Yong-Sang, J.; Meilhac, O.; Jestin, E. Regioselectivity of thiouracil alkylation: Application to optimization of Darapladib synthesis, *Bioorg. Med. Chem. Lett.* **2017**, *28* (4), 787-792.
33. Mossine, A. V.; Brooks, A. F.; Bernard-Gauthier, V.; Bailey, J. J.; Ichiishi, N.; Schirrmacher, R.; Sanford, M. S.; Scott, P. J. H. Automated synthesis of PET radiotracers by copper-mediated 18 F-fluorination of organoborons: Importance of the order of addition and competing protodeborylation, *J. Labelled Compd. Radiopharm.*, **2018**, *61* (3), 228-236.
34. Rudd, J. H.; Myers, K. S.; Bansilal, S.; Machac, J.; Pinto, C. A.; Tong, C.; Rafique, A.; Hargeaves, R.; Farkouh, M.; Fuster, V.; Fayad, Z. A. Atherosclerosis Inflammation Imaging with 18F-FDG PET: Carotid, Iliac, and Femoral Uptake Reproducibility, Quantification Methods, and Recommendations, *J. Nucl. Med.* **2008**, *49* (6), 871-878.
35. Dave, M.; Nash, M.; Young, G. C.; Ellens, H.; Magee, M. H.; Roberts, A. D.; Taylor, M. A.; Greenhill, R. W.; Boyle, G. W. Disposition and Metabolism of Darapladib, a Lipoprotein-Associated Phospholipase A2 Inhibitor, in Humans, *Drug Metabol. Dispos.* **2014**, *42* (3), 415-430.
36. Leclercq, A.; Houarda, X.; Loyau, S.; Philippe, M.; Sebbagd, U.; Meilhac, O.; Michel, J.B. Topology of protease activities reflects atherothrombotic plaque complexity, *Atherosclerosis*, **2007**, 191 (1), 1-10.
37. Banciu, M.; Metselaar, J. M.; Schiffelers, R. M.; Storm, G. Antitumor Activity of Liposomal Prednisolone Phosphate Depends on the Presence of Functional Tumor-Associated Macrophages in Tumor Tissue, *Neoplasia*, **2008**, *10*(2), 108-17.

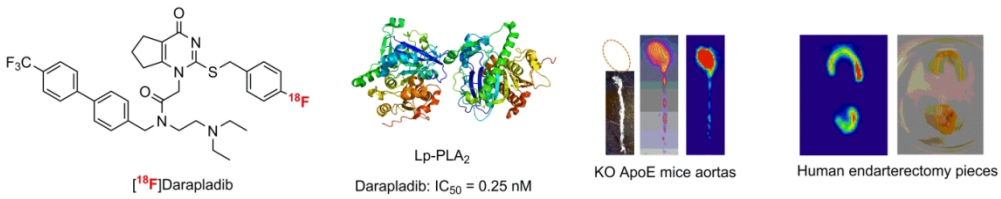

366x72mm (96 x 96 DPI)